Alkyl Transfer to Metal Thiolates: Kinetics, Active Species Identification, and Relevance to the DNA Methyl Phosphotriester Repair Center of *Escherichia coli* Ada

Jonathan J. Wilker and Stephen J. Lippard*

Department of Chemistry, Massachusetts Institute of Technology, Cambridge, Massachusetts 02139

Received September 6, 1996[⊗]

The Ada protein of *Escherichia coli* employs a $[Zn(S\text{-cys})_4]^{2-}$ site to repair deoxyribonucleic acid alkyl phosphotriester lesions. The alkyl group is transferred to a cysteine thiolate in a stoichiometric reaction. We describe a functional model for this chemistry in which a thiolate of $[(CH_3)_4N]_2[Zn(SC_6H_5)_4]$ accepts a methyl group from $(CH_3O)_3PO$. The thiolate salt $(CH_3)_4N(SC_6H_5)$ is also active in methyl transfer, but the thiol C_6H_5SH fails to react. Conductivity measurements and kinetic studies demonstrate that $[(CH_3)_4N]_2[Zn(SC_6H_5)_4]$ forms ion pairs in dimethyl sulfoxide (DMSO) solution ($K_{IP} = 13 \pm 4\ M^{-1}$) which exhibit diminished reactivity. The reaction of $[Zn(SC_6H_5)_4]^{2-}$ with $(CH_3O)_3PO$ is first order with respect to each reagent. A second-order rate constant for this reaction, k_{Zn}, was determined to be $(1.6 \pm 0.3) \times 10^{-2}\ M^{-1}\ s^{-1}$. From kinetic data and equilibria studies, all reactivity of $[(CH_3)_4N]_2[Zn(SC_6H_5)_4]$ toward $(CH_3O)_3PO$ could be attributed to dissociated thiolate. Metal complexes representing alternative protein sites were prepared and displayed the following kinetic trend of methyl transfer ability: $[(CH_3)_4N]_2[Zn(SC_6H_5)_4] > [(CH_3)_4N]_2[Co(SC_6H_5)_4] \approx [(CH_3)_4N]_2[Cd(SC_6H_5)_4] > [(CH_3)_4N][Zn(SC_6H_5)_3(MeIm)] > [Zn(SC_6H_5)_2(MeIm)_2]$, where MeIm = 1-methylimidazole. These results are consistent with a dissociated thiolate being the active species and suggest that a similar mechanism might apply to alkyl phosphotriester repair by Ada.

Introduction

Proteins capable of repairing DNA alkylation damage occur in most organisms.[1−3] One of the best studied examples is the Ada protein of *Escherichia coli*. Ada is responsible for repair of O^6-alkylguanine, O^4-alkylthymine, and the S_p diastereomer of alkyl phosphotriesters.[4−6] The lesions are repaired by stoichiometric and irreversible transfer of the offending alkyl group to cysteine residues of the protein.[4,6−12] Separate active sites are present for mending the two alkylation damage types.[4,10,11] Base alkylation is repaired in the C-terminal portion of Ada by Cys321,[7,11,12] which is embedded in the sequence Asn-X_6-Pro-Cys-His-Arg-Val-X_9-Tyr-$X_{13/14}$-Glu, conserved by all known O^6-alkylguanine transferases.[13] This repair process does not require a metal ion. Phosphate damage is repaired by alkyl transfer to Cys69,[10,11] one of four cysteine residues bound to a zinc ion in the N-terminus of Ada.[8,14−16]

The use of a $[Zn(S\text{-cys})_4]^{2-}$ site to repair alkyl phosphotriesters raises several questions for the inorganic chemist. Why is Cys69, the residue responsible for repair, coordinated to zinc? Why does the ligand environment of this zinc ion comprise four cysteine residues? When the cysteine thiolate accepts an alkyl group from an alkyl phosphotriester, is it coordinated to zinc or transiently dissociated? How does the nucleophilicity of a metal thiolate compare to that of the analogous thiolate alone? Why was zinc selected over other metal ions?

Previously, we used $[(CH_3)_4N]_2[Zn(SC_6H_5)_4]$ to mimic the $[Zn(S\text{-cys})_4]^{2-}$ site of Ada and $(CH_3O)_3PO$ to represent a DNA methyl phosphotriester lesion in a functional model system.[17] Methyl transfer from $(CH_3O)_3PO$ to a thiolate of $[(CH_3)_4N]_2[Zn(SC_6H_5)_4]$ occurred in deuterated dimethyl sulfoxide (DMSO-d_6) solution, but zinc was not required for this reaction. Methyl transfer from $(CH_3O)_3PO$ to benzenethiolate, $(CH_3)_4N(SC_6H_5)$, readily took place. The analogous thiol, C_6H_5SH, however, was unreactive toward $(CH_3O)_3PO$. We concluded that zinc coordination of Cys69 maintains its thiolate activity in alkyl phosphotriester repair, preventing protonation and inactivation by accessible water.

In the present report, we further analyze the reaction between $[(CH_3)_4N]_2[Zn(SC_6H_5)_4]$ and $(CH_3O)_3PO$ in DMSO. Included in this analysis are the order dependencies of each reagent to provide an overall rate equation, characterization of ion pairing and ligand dissociation processes, and consideration of whether or not the thiolate accepting a methyl group from $(CH_3O)_3PO$ is bound to zinc. We also explore the methyl transfer properties of cobalt(II) and cadmium(II) tetrathiolate analogs and of model compounds representing $[Zn(S\text{-cys})_3(N\text{-his})]^-$ and $[Zn(S\text{-cys})_2$-

[⊗] Abstract published in *Advance ACS Abstracts,* February 1, 1997.

(1) Friedberg, E. C.; Walker, G. C.; Siede, W. *DNA Repair and Mutagenesis*; ASM Press: Washington DC, 1995.
(2) Friedberg, E. C. *BioEssays* **1994**, *16*, 645−649.
(3) Lindahl, T. *Nature* **1993**, *362*, 709−715.
(4) McCarthy, T. V.; Lindahl, T. *Nucl. Acid Res.* **1985**, *13*, 2683−2698.
(5) Teo, I.; Sedgwick, B.; Demple, B.; Li, B.; Lindahl, T. *EMBO J.* **1984**, *3*, 2151−2157.
(6) Demple, B.; Jacobsson, A.; Olsson, M.; Robins, P.; Lindahl, T. *J. Biol. Chem.* **1982**, *257*, 13776−13780.
(7) Moore, M. H.; Gulbis, J. M.; Dodson, E. J.; Demple, B.; Moody, P. C. E. *EMBO J.* **1994**, *13*, 1495−1501.
(8) Myers, L. C.; Cushing, T. D.; Wagner, G.; Verdine, G. L. *Chem. Biol.* **1994**, *1*, 91−97.
(9) Ohkubo, T.; Sakashita, H.; Sakuma, T.; Kainosho, M.; Sekiguchi, M.; Morikawa, K. *J. Am. Chem. Soc.* **1994**, *116*, 6035−6036.
(10) Sedgwick, B.; Robins, P.; Totty, N.; Lindahl, T. *J. Biol. Chem.* **1988**, *263*, 4430−4433.
(11) Takano, K.; Nakabeppu, Y.; Sekiguchi, M. *J. Mol. Biol.* **1988**, *201*, 261−271.
(12) Demple, B.; Sedgwick, B.; Robins, P.; Totty, N.; Waterfield, M. D.; Lindahl, T. *Proc. Natl. Acad. Sci. U.S.A.* **1985**, *82*, 2688−2692.
(13) Wibley, J. E. A.; McKie, J. H.; Embrey, K.; Marks, D. S.; Douglas, K. T.; Moore, M. H.; Moody, P. C. E. *Anti-Cancer Drug Des.* **1995**, *10*, 75−95.
(14) Myers, L. C.; Terranova, M. P.; Ferentz, A. E.; Wagner, G.; Verdine, G. L. *Science* **1993**, *261*, 1164−1167.
(15) Myers, L. C.; Verdine, G. L.; Wagner, G. *Biochemistry* **1993**, *32*, 14089−14094.
(16) Myers, L. C.; Terranova, M. P.; Nash, H. M.; Markis, M. A.; Verdine, G. L. *Biochemistry* **1992**, *31*, 4541−4547.
(17) Wilker, J. J.; Lippard, S. J. *J. Am. Chem. Soc.* **1995**, *117*, 8682−8683.

S0020-1669(96)01082-8 CCC: $14.00

Table 1. Pseudo-First-Order Rate Constants for Reactions of Benzenethiolate and Its Metal Complexes with $(CH_3O)_3PO$[a]

compound	k (s^{-1})
$[(CH_3)_4N]_2[Zn(SC_6H_5)_4]$	$(8.2 \pm 0.6) \times 10^{-5}$
$[(CH_3)_4N][Zn(SC_6H_5)_3(MeIm)]$	$(6 \pm 1) \times 10^{-6}$
$[Zn(SC_6H_5)_2(MeIm)_2]$	$\leq 5 \times 10^{-8}$
$(CH_3)_4N(SC_6H_5)$	$(1.1 \pm 0.3) \times 10^{-4}$
$[(CH_3)_4N]_2[Co(SC_6H_5)_4]$	$(4 \pm 1) \times 10^{-5}$
$[(CH_3)_4N]_2[Cd(SC_6H_5)_4]$	$(3 \pm 1) \times 10^{-5}$

[a] Reactions were carried out with 5.0 mM thiolate or metal complex and 1.0 mM $(CH_3O)_3PO$ in DMSO-d_6. With the exception of $[Zn(SC_6H_5)_2(MeIm)_2]$, all rate constants shown are an average of three kinetic runs. Error estimates reflect 1 standard deviation.

(N-his)$_2$] protein sites. The general nucleophilic character of free vs metal-bound thiolates is discussed.

Experimental Section

General Procedures. All procedures were carried out under an argon or nitrogen atmosphere using standard Schlenk and glovebox techniques. Solvents were dried, degassed, and distilled according to standard procedures.[18,19] NMR spectra were recorded at 25 ± 1 °C on Varian Unity 300 and VXR-500 instruments. All $^{31}P\{^1H\}$ NMR spectra were recorded on samples with phosphorus concentrations of 211 mM. For solubility reasons, all NMR spectra were taken in DMSO-d_6. The parent complex $[(CH_3)_4N]_2[Zn(SC_6H_5)_4]$ was synthesized according to a literature procedure.[20] The compounds $[(CH_3)_4N][Zn(SC_6H_5)_3(MeIm)]$ and $[Zn(SC_6H_5)_2(MeIm)_2]$ were prepared as reported previously.[17]

Kinetics. All kinetic runs were performed under pseudo-first-order conditions with the concentration of thiolate or metal thiolate in excess over $(CH_3O)_3PO$ to prevent more than 1 equiv of methyl transfer. Reaction kinetics were monitored by ^1H NMR spectroscopy in DMSO-d_6 at 24.5 (± 0.6) °C. Typical ^1H NMR parameters for kinetic studies included 4 scans per spectrum, 40 s relaxation delay between scans, and 60 spectra per experiment. The total time of data collection was 6 h. Solution volumes were standardized by using calibrated 1 mL volumetric flasks. Concentrations of reactants and products were determined by referencing peak integrals to the methyl resonances of $(CH_3)_4N^+$ counterions, the concentration of which was determined from starting material quantities and known solution volumes. Rate constants were determined by curve fitting $(CH_3O)_3PO$ concentration-vs-time plots with a standard, integrated expression for first-order decay.[21] Pseudo-first-order rate constants (Table 1) were determined in triplicate, and the reported values are averages of the three kinetic runs with errors reflecting one standard deviation.

Conductivity. Conductivity measurements were recorded on a Fisher Scientific Model 09-326 conductivity meter equipped with a platinum electrode. The instrument response was calibrated with NIST conductivity calibration standards of KCl purchased from Fisher Scientific. All solution temperatures were 24 ± 1 °C.

$(CH_3)_4N(SC_6H_5)$. Benzenethiol (13.3 g, 121 mmol) was added to an ethanol (50 mL) solution of $(CH_3)_4N(OH)\cdot 5H_2O$ (21.8 g, 120 mmol). The solvent was removed under vacuum to yield a colorless solid that was recrystallized from boiling acetonitrile. ^1H NMR (DMSO-d_6): δ 3.08 (s, 12 H, $(CH_3)N^+$), 6.40 (t, 1 H, *p*-H), 6.64 (t, 2 H, *m*-H), 7.00 (d, 2 H, *o*-H). Anal. Calcd for $C_{10}H_{17}NS$: C, 65.52; H, 9.35; N, 7.64. Found: C, 65.83; H, 9.66; N, 7.91.

$[(CH_3)_4N]_2[Co(SC_6H_5)_4]$. This compound was prepared by modification of a literature procedure.[22] A methanol (40 mL) solution of $Co(NO_3)_2\cdot 6H_2O$ (8.74 g, 30.0 mmol) was added to a methanol (80 mL) solution of C_6H_5SH (22.9 g, 208 mmol), $(C_2H_5)_3N$ (21.0 g, 208 mmol), and $(CH_3)_4NCl$ (7.50 g, 68.3 mmol) over 45 min with stirring. Addition of 2-propanol (45 mL) and overnight storage at −20 °C provided green crystals (9.08 g, 14.1 mmol, 47%) which were collected by filtration, washed with 2-propanol, and dried in vacuo. Anal. Calcd for $C_{32}H_{44}N_2S_4Co$: C 59.69; H, 6.89; N, 4.35. Found: C, 59.21; H, 6.88; N, 4.28.

$[(CH_3)_4N]_2[Cd(SC_6H_5)_4]$. A literature synthesis was modified to obtain this complex.[20] Benzenethiol (8.91 g, 80.9 mmol), $(C_4H_9)_3N$ (12.5 g, 124 mmol), and $(CH_3)_4NCl$ (5.51 g, 50.3 mmol) were combined in methanol (175 mL). To this solution was added $Cd(NO_3)_2\cdot 4H_2O$ (2.58 g, 8.36 mmol) in methanol (25 mL) over 2 h. Normal butanol (125 mL) was added over 10 min, and the reaction solution was stored at −20 °C overnight. The resulting colorless crystals were collected, washed with *n*-C_4H_9OH, and dried in vacuo. These crystals were recrystallized from CH_3CN (50 mL), collected by filtration, washed with *n*-C_4H_9OH, and dried in vacuo. ^1H NMR (DMSO-d_6): δ 3.05 (s, 24 H, $(CH_3)N^+$), 6.62 (t, 4 H, *p*-H), 6.75 (t, 8 H, *m*-H), 7.36 (d, 8 H, *o*-H). Anal. Calcd for $C_{32}H_{44}N_2S_4Cd$: C, 55.11; H, 6.36; N, 4.02. Found: C, 55.02; H, 6.33; N, 4.02.

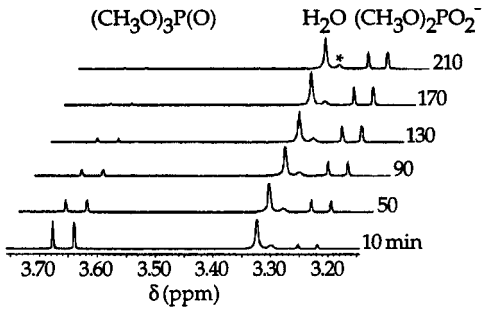

Figure 1. Aliphatic region ^1H NMR spectral changes used to follow the stoichiometric reaction of $[(CH_3)_4N]_2[Zn(SC_6H_5)_4]$ and $(CH_3O)_3PO$ in DMSO-d_6. The reaction was run under pseudo-first-order conditions with excess $[(CH_3)_4N]_2[Zn(SC_6H_5)_4]$. The asterisk indicates a signal arising from $^{13}C-^1H$ coupling of the $(CH_3)_4N^+$ counterion.

Results

Reaction of $[(CH_3)_4N]_2[Zn(SC_6H_5)_4]$ with $(CH_3O)_3PO$. As shown by time-dependent ^1H NMR spectroscopy in Figure 1, a 1:1 mixture of $[(CH_3)_4N]_2[Zn(SC_6H_5)_4]$ and $(CH_3O)_3PO$ in DMSO-d_6 reacts quantitatively to form $CH_3SC_6H_5$, $(CH_3O)_2PO_2^-$, and $\{Zn(SC_6H_5)_3\}^-$. The $CH_3SC_6H_5$ product is not coordinated to zinc as evidenced by the fact that its ^1H NMR resonances are identical to those of an authentic sample. The zinc-containing reaction product retains three bound thiolates, which are equivalent by ^1H NMR spectroscopy. The $^{31}P\{^1H\}$ NMR peak of $(CH_3O)_2PO_2^-$ is broad ($\Delta\nu_{1/2} = 60$ Hz) relative to that of a genuine sample of $(NH_4)[(CH_3O)_2PO_2]$ ($\Delta\nu_{1/2} = 5.1$ Hz). Owing to the high freezing point of DMSO-d_6 (18 °C), we were unable to cool the NMR sample significantly. Heating the reaction solution, however, sharpens $^{31}P\{^1H\}$ NMR lines of the $(CH_3O)_2PO_2^-$ product. From these results, we conclude that $(CH_3O)_2PO_2^-$ is in dynamic equilibrium between zinc-bound and free states. Scheme 1 depicts the reaction between $[(CH_3)_4N]_2[Zn(SC_6H_5)_4]$ and $(CH_3O)_3PO$. Attempts to crystallize the zinc-containing reaction product from DMSO solutions for single-crystal X-ray structural analysis afforded only crystals of $[(CH_3)_4N]_2[Zn(SC_6H_5)_4]$.

A kinetic analysis was undertaken to understand better methyl transfer from $(CH_3O)_3PO$ to $[(CH_3)_4N]_2[Zn(SC_6H_5)_4]$. As shown in Figure 2, the reaction is first order in $(CH_3O)_3PO$. By maintaining the $(CH_3O)_3PO$ concentration at a constant value of 8.5 mM and varying $[(CH_3)_4N]_2[Zn(SC_6H_5)_4]$ from 30.0 to 181, mM, we obtained data for a plot of pseudo-first-order rate constant (k_{obs}) vs $[(CH_3)_4N]_2[Zn(SC_6H_5)_4]$ concentration (Figure 3). At higher concentrations of zinc, fewer data points were

(18) Perrin, D. D.; Armarego, W. L. F. *Purification of Laboratory Chemicals*; Third ed.; Butterworth-Heinemann Ltd.: Boston, MA, 1988.
(19) Gordon, A. J.; Ford, R. A. *The Chemist's Companion. A Handbook of Practical Data, Techniques, and References*; John Wiley and Sons: New York, 1972.
(20) Dance, I. G.; Choy, A.; Scudder, M. L. *J. Am. Chem. Soc.* **1984**, *106*, 6285−6295.
(21) Wilkins, R. G. *Kinetics and Mechanism of Reactions of Transition Metal Complexes*; 2nd ed.; VCH Publishers Inc.: New York, 1991.
(22) Dance, I. G. *J. Am. Chem. Soc.* **1979**, *101*, 6264−6273.

Scheme 1

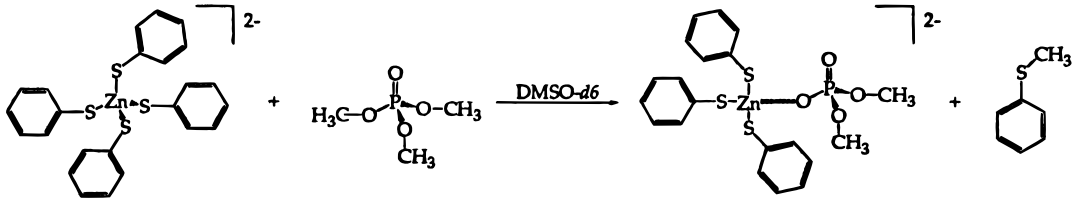

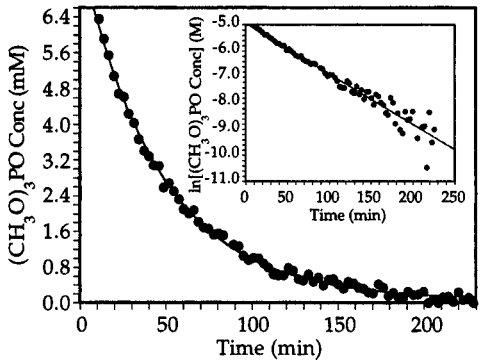

Figure 2. $(CH_3O)_3PO$ concentration vs time plot for a typical kinetic run of the reaction between $[(CH_3)_4N]_2[Zn(SC_6H_5)_4]$ and $(CH_3O)_3PO$. Pseudo-first-order conditions with $[(CH_3)_4N]_2[Zn(SC_6H_5)_4]$ in excess were employed. The data are fit to a first-order decay. The inset displays the natural log of $(CH_3O)_3PO$ concentration plotted against time. These data are fit to a line.

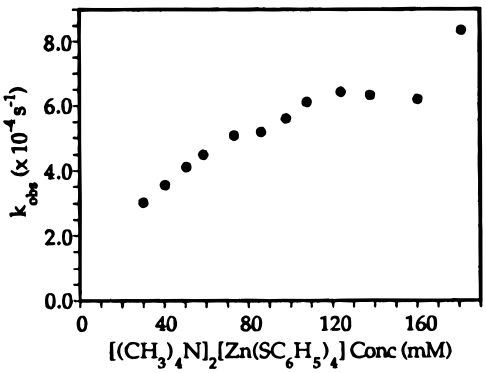

Figure 3. k_{obs} vs $[(CH_3)_4N]_2[Zn(SC_6H_5)_4]$ concentration plot. The $(CH_3O)_3PO$ concentration remained constant at 8.5 mM and $[(CH_3)_4N]_2[Zn(SC_6H_5)_4]$ concentration was varied over the range indicated.

available in plots of the $(CH_3O)_3PO$ concentration vs time required to obtain rate constants, leading to larger intrinsic errors. Nevertheless, a leveling off in k_{obs} is apparent, suggesting the formation of $\{[(CH_3)_4N][Zn(SC_6H_5)_4]\}^-$ ion pairs.

Ion Pairing. The conductivity of $[(CH_3)_4N]_2[Zn(SC_6H_5)_4]$ in DMSO solution further indicated the presence of ion pairing, as revealed by curvature in the plot with increasing $[(CH_3)_4N]_2[Zn(SC_6H_5)_4]$ concentration (Figure 4). In order to evaluate the effect of ion pairing on the reaction of $[(CH_3)_4N]_2[Zn(SC_6H_5)_4]$ with $(CH_3O)_3PO$, we performed kinetic studies in the presence of added $(CH_3)_4N(PF_6)$ to increase the concentration of the ion paired species $\{[(CH_3)_4N][Zn(SC_6H_5)_4]\}^-$. The k_{obs} values were diminished relative to those obtained in analogous runs without added $(CH_3)_4N(PF_6)$ (data not shown).

A model was formulated to describe the effect of ion pairing on the methyl transfer reaction. This model separates the reactivity of $[Zn(SC_6H_5)_4]^{2-}$ from that of the ion paired species $\{[(CH_3)_4N][Zn(SC_6H_5)_4]\}^-$. As shown in Scheme 2, the model proposes that $[Zn(SC_6H_5)_4]^{2-}$ is competent to react with $(CH_3O)_3PO$ but the less charged $\{[(CH_3)_4N][Zn(SC_6H_5)_4]\}^-$ is not. This assumption is consistent with the observation that the reaction of $[Zn(SC_6H_5)_3(MeIm)]^-$ with $(CH_3O)_3PO$ has a pseudo-first-order rate constant an order of magnitude lower than that of $[Zn(SC_6H_5)_4]^{2-}$ (Table 1).

We designate the concentration of $[Zn(SC_6H_5)_4]^{2-}$, solvated but not ion paired, as $[\{Zn(SC_6H_5)_4\}^{2-}]_{free}$; the concentration of $(CH_3)_4N^+$ not involved in ion pairing as $[(CH_3)_4N^+]_{free}$; and the concentration of ion-paired zinc species as $[\{[(CH_3)_4N][Zn(SC_6H_5)_4]\}^-]$. The equilibrium constant for ion pairing, K_{IP}, is defined in eq 1 and the total zinc in eq 2. The

$$K_{IP} = \frac{[\{(CH_3)_4][Zn(SC_6H_5)_4]\}^-]}{[\{Zn(SC_6H_5)_4{}^{2-}\}]_{free}[(CH_3)_4N^+]_{free}} \quad (1)$$

$$[Zn^{2+}]_{tot} = [\{Zn(SC_6H_5)_4\}^{2-}]_{free} + [\{[(CH_3)_4N][Zn(SC_6H_5)_4]\}^-] \quad (2)$$

observed pseudo-first-order rate constant for the reaction of $[(CH_3)_4N]_2[Zn(SC_6H_5)_4]$ with $(CH_3O)_3PO$, k_{obs}, is the product of the true second-order rate constant, k_{Zn}, and $[\{Zn(SC_6H_5)_4\}^{2-}]_{free}$ (eq 3). Equations 1−3 can be rearranged

$$k_{obs} = k_{Zn}[\{Zn(SC_6H_5)_4\}^{2-}]_{free} \quad (3)$$

to provide an expression for $[(CH_3)_4N^+]_{free}$ in terms of k_{Zn}, k_{obs}, K_{IP}, and $[Zn^{2+}]_{tot}$ (eq 4 derived in Appendix S1; see Supporting

$$[(CH_3)_4N^+]_{free} = \frac{k_{Zn}[Zn^{2+}]_{tot} - k_{obs}}{K_{IP}k_{obs}} \quad (4)$$

Information). From eq 4, it is clear that a plot of $[Zn^{2+}]_{tot}/k_{obs}$ vs $[(CH_3)_4N^+]_{free}$ yields a slope of K_{IP}/k_{Zn} and an ordinate intercept of $1/k_{Zn}$. This plot thus affords both K_{IP} and k_{Zn} if the $(CH_3)_4N^+_{free}$ concentrations are known.

The $(CH_3)_4N^+_{free}$ concentrations were obtained by the following iterative procedure. For each $[(CH_3)_4N]_2[Zn(SC_6H_5)_4]$ concentration at which a kinetic run was performed (Figure 3), an initial guess of $[(CH_3)_4N^+]_{free}$ was made. Plotting $[Zn^{2+}]_{tot}/k_{obs}$ vs $[(CH_3)_4N^+]_{free}$ provided a rough estimate of the ion pairing equilibrium constant, K_{IP}, and the second-order rate constant, k_{Zn}, from eq 4. By using eqs 1 and 2, substitution and rearrangement afforded an expression for $[(CH_3)_4N^+]_{free}$ in terms only of K_{IP} and $[Zn^{2+}]_{tot}$ (eq 5, derived in Appendix S2).

$$[(CH_3)_4N^+]_{free} = \frac{K_{IP}[Zn^{2+}]_{tot} - 1 \pm ((K_{IP}[Zn^{2+}]_{tot})^2 + 6K_{IP}[Zn^{2+}]_{tot} + 1)^{1/2}}{2K_{IP}} \quad (5)$$

The initial K_{IP} value was used in eq 5 to estimate the $(CH_3)_4N^+_{free}$ concentrations. Replotting $[Zn^{2+}]_{tot}/k_{obs}$ vs $[(CH_3)_4N^+]_{free}$ yielded superior K_{IP} and k_{Zn} values. This process was repeated until the $[(CH_3)_4N^+]_{free}$, K_{IP}, and k_{Zn} values converged. The final iteration of such a $[Zn^{2+}]_{tot}/k_{obs}$ vs $[(CH_3)_4N^+]_{free}$ plot is shown in Figure 5. From the ordinate intercept, we obtained a second-order rate constant for the

Scheme 2

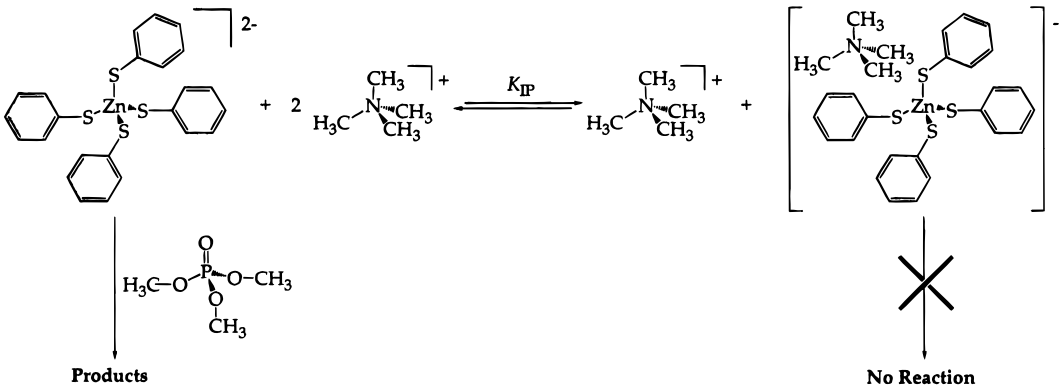

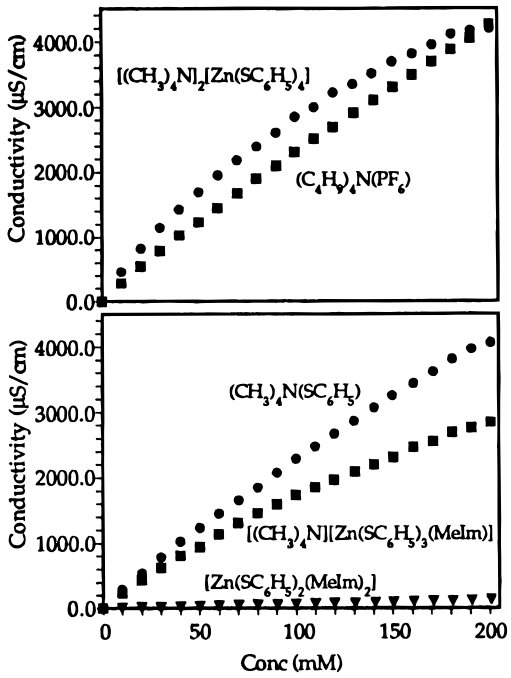

Figure 4. Conductivity vs concentration plots of $[(CH_3)_4N]_2[Zn(SC_6H_5)_4]$ (top), $(C_4H_9)_4N(PF_6)$ (top), $[(CH_3)_4N][Zn(SC_6H_5)_3(MeIm)]$ (bottom), $[Zn(SC_6H_5)_2(MeIm)_2]$ (bottom), and $(CH_3)_4N(SC_6H_5)$ (bottom) in DMSO.

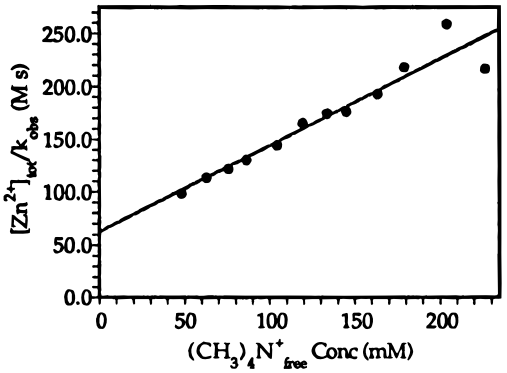

Figure 5. Final iteration of the $[Zn^{2+}]_{tot}/k_{obs}$ vs $[(CH_3)_4N^+_{free}]$ plots with a linear fit. The inverse ordinate intercept affords a second-order rate constant, k_{Zn}, of $(1.6 \pm 0.3) \times 10^{-2}$ M^{-1} s^{-1}. The slope of K_{IP}/k_{Zn} yields an ion pairing equilibrium constant, K_{IP}, of 13 ± 4 M^{-1}.

reaction of $[Zn(SC_6H_5)_4]^{2-}$ and $(CH_3O)_3PO$ of $(1.6 \pm 0.3) \times 10^{-2}$ M^{-1} s^{-1} (Table 2). This plot also afforded an ion pairing equilibrium constant, K_{IP}, of 13 ± 4 M^{-1} (Table 2).

With this value of K_{IP}, the exact concentration of $[\{Zn(SC_6H_5)_4\}^{2-}]_{free}$ available for reaction with $(CH_3O)_3PO$ is known for any starting $[(CH_3)_4N]_2[Zn(SC_6H_5)_4]$ concentration. A plot of k_{obs} vs $[\{Zn(SC_6H_5)_4\}^{2-}]_{free}$ concentration provided the reaction order dependence on $[\{Zn(SC_6H_5)_4\}^{2-}]_{free}$. As shown in Figure 6, this plot gave a straight line with an intercept at the origin. From the plot, we conclude that the reaction of $[Zn(SC_6H_5)_4]^{2-}$ and $(CH_3O)_3PO$ is first order with respect to $[\{Zn(SC_6H_5)_4\}^{2-}]_{free}$ concentration. With the order dependencies of both reagents known, we arrived at the final rate equation for the reaction of $[(CH_3)_4N]_2[Zn(SC_6H_5)_4]$ and $(CH_3O)_3PO$, eq 6.

$$-\frac{d[\{Zn(SC_6H_5)_4\}^{2-}]}{dt} = k_{Zn}[\{Zn(SC_6H_5)_4\}^{2-}][(CH_3O)_3PO] \quad (6)$$

Ligand Dissociation. We next address the question of whether the active species is a zinc-bound or free thiolate.

Table 2. Summary of Equilibrium and Rate Constants Discussed in the Text

constant	value
k_{Zn} (M^{-1} s^{-1})	$(1.6 \pm 0.3) \times 10^{-2}$
K_{IP} (M^{-1})	13 ± 4
$K_{DissocIP}$ (M)	$(1.0 \pm 0.9) \times 10^{-2}$
K_{Dissoc} (M)	$> (1.0 \pm 0.9) \times 10^{-2}$
k_{PhS} (M^{-1} s^{-1})	$(2.2 \pm 0.6) \times 10^{-2}$
k_{calc} (s^{-1})	$(8 \pm 4) \times 10^{-5}$

Equation 7 describes situations in which the observed reactivity

$$k_{obs} = k_{Zn}[\{Zn(SC_6H_5)_4\}^{2-}]_{free} + k_{PhS}[C_6H_5S^-] \quad (7)$$

of $[(CH_3)_4N]_2[Zn(SC_6H_5)_4]$, parametrized by k_{obs}, can be ascribed exclusively to zinc-bound thiolate, completely dissociated thiolate, or a combination of the two. In this equation, the second-order rate constant for reaction of dissociated benzenethiolate is k_{PhS}. To discern the relative contributions of $[Zn(SC_6H_5)_4{}^{2-}]_{free}$ and $C_6H_5S^-$ to the $[(CH_3)_4N]_2[Zn(SC_6H_5)_4]$ reactivity, the concentrations of each species are required.

Figure 7 displays the aromatic region of the ^1H NMR spectra of $(CH_3)_4N(SC_6H_5)$, $[(CH_3)_4N]_2[Zn(SC_6H_5)_4]$, $[(CH_3)_4N][Zn(SC_6H_5)_3(MeIm)]$, and $[Zn(SC_6H_5)_2(MeIm)_2]$ in DMSO-d_6. For $(CH_3)_4N(SC_6H_5)$, the peaks are sharp with well-resolved spin−spin coupling. For $[(CH_3)_4N]_2[Zn(SC_6H_5)_4]$, however, they are broad and display almost no splitting. The spectra of $[(CH_3)_4N][Zn(SC_6H_5)_3(MeIm)]$ and $[Zn(SC_6H_5)_2(MeIm)_2]$ are sharper and have better resolved spin−spin coupling. Ligand dissociation accounts for the line broadening trend of $[Zn(SC_6H_5)_4]^{2-}$ > $[Zn(SC_6H_5)_3(MeIm)]^-$ > $[Zn(SC_6H_5)_2(MeIm)_2]$. The $[Zn(SC_6H_5)_4]^{2-}$ dianion is expected to dissociate a thiolate ligand more readily than $[Zn(SC_6H_5)_3(MeIm)]^-$. Neutral $[Zn(SC_6H_5)_2(MeIm)_2]$ is even less likely to dissociate such a ligand. The

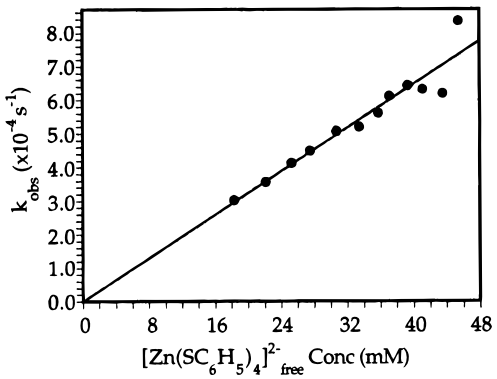

Figure 6. k_{obs} vs $[\{Zn(SC_6H_5)_4\}^{2-}]_{free}$ concentration plot with a linear fit indicating a first-order dependence of the reaction between $[(CH_3)_4N]_2[Zn(SC_6H_5)_4]$ and $(CH_3O)_3PO$ on $[\{Zn(SC_6H_5)_4\}^{2-}]_{free}$ concentration.

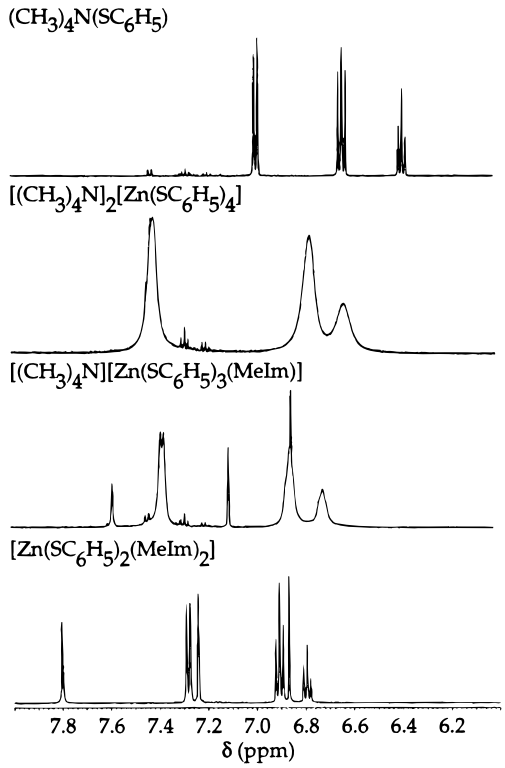

Figure 7. Aromatic region ^1H NMR spectra of $(CH_3)_4N(SC_6H_5)$, $[(CH_3)_4N]_2[Zn(SC_6H_5)_4]$, $[(CH_3)_4N][Zn(SC_6H_5)_3(MeIm)]$, and $[Zn(SC_6H_5)_2(MeIm)_2]$ in DMSO-d_6.

results in Figure 7 indicate that the rate of ligand dissociation, as measured by line widths, increases with increasing thiolate content of the complexes. Since the exchange is fast on the ^1H NMR time scale, we cannot determine from these data alone the extent of ligand dissociation by integrating peaks associated with the zinc-bound and dissociated benzenethiolate. On the other hand, the rapid exchange permits us to discount ligand dissociation as a rate-determining step in the reaction of $[(CH_3)_4N]_2[Zn(SC_6H_5)_4]$ with $(CH_3O)_3PO$, owing to the low rate constants of methyl transfer (Table 1).

Scheme 3 depicts the consequences of ligand dissociation on the reaction of non-ion-paired $[Zn(SC_6H_5)_4]^{2-}$ with $(CH_3O)_3PO$. Free benzenethiolate will react with $(CH_3O)_3PO$ as indicated (Table 1). Although the identity of the zinc species following thiolate dissociation is unknown, solvent binding to the empty coordination site is likely. The resulting zinc species will have one less negative charge compared to $[Zn(SC_6H_5)_4]^{2-}$. We assume reactivity of the solvated species $[Zn(SC_6H_5)_3(DMSO)]^-$ to be negligible relative to $[Zn(SC_6H_5)_4]^{2-}$ and $C_6H_5S^-$. The extent of ligand dissociation is defined by an equilibrium constant, K_{Dissoc}, given in eq 8.

$$K_{Dissoc} = \frac{[\{Zn(SC_6H_5)_3(DMSO)\}^-][C_6H_5S^-]}{[\{Zn(SC_6H_5)_4\}^{2-}]_{free}} \quad (8)$$

Combined Effects of Ion Pairing and Ligand Dissociation. In order to define completely the reactivity of $[(CH_3)_4N]_2[Zn(SC_6H_5)_4]$ in DMSO, knowledge of both ion pairing and ligand dissociation processes is required. The extent of $[Zn(SC_6H_5)_3(DMSO)]^-$ ion pairing will be significantly less than that of $[Zn(SC_6H_5)_4]^{2-}$ owing to the reduced charge. In addition, the ion-paired product $\{[(CH_3)_4N][Zn(SC_6H_5)_4]\}^-$ can dissociate a thiolate ligand. Scheme 4 depicts these possibilities. With $[(CH_3)_4N^+]_{free}$ representing the concentration of tetramethylammonium ion not involved in ion pairing, the equilibrium constant for ligand dissociation from the ion paired complex $\{[(CH_3)_4N][Zn(SC_6H_5)_4]\}^-$, $K_{DissocIP}$, is given by eq 9. Dissociation of the anionic benzenethiolate ligand will occur more readily from $[Zn(SC_6H_5)_4]^{2-}$ than $\{[(CH_3)_4N][Zn(SC_6H_5)_4]\}^-$ because of its greater negative charge. The equilibrium constant for dissociation from $[Zn(SC_6H_5)_4]^{2-}$, K_{Dissoc}, will therefore be greater than from $\{[(CH_3)_4N][Zn(SC_6H_5)_4]\}^-$, $K_{DissocIP}$ (eq 10).

$$K_{DissocIP} = \frac{[\{Zn(SC_6H_5)_3(DMSO)\}^-][C_6H_5S^-][(CH_3)_4N^+]_{free}}{[\{[(CH_3)_4N][Zn(SC_6H_4)_4]\}^-]} \quad (9)$$

$$K_{Dissoc} > K_{DissocIP} \quad (10)$$

As depicted in Scheme 4, addition of $(CH_3)_4N^+$ to a solution of $[Zn(SC_6H_5)_4]^{2-}$ will shift the ion-pairing equilibrium toward $\{[(CH_3)_4N][Zn(SC_6H_5)_4]\}^-$. Addition of $C_6H_5S^-$ to a DMSO solution containing the ligand-dissociated complex $[Zn(SC_6H_5)_3(DMSO)]^-$ will convert this complex into the two forms of zinc tetrathiolate, $[Zn(SC_6H_5)_4]^{2-}$ and $\{[(CH_3)_4N][Zn(SC_6H_5)_4]\}^-$. In order to drive experimentally these solution equilibria toward the ion-paired tetrathiolate, $\{[(CH_3)_4N][Zn(SC_6H_5)_4]\}^-$, both $(CH_3)_4N^+$ and $C_6H_5S^-$, in the form of $(CH_3)_4N(SC_6H_5)$, were added to DMSO-d_6 solutions of $[(CH_3)_4N]_2[Zn(SC_6H_5)_4]$ at varying ratios. While keeping the concentration of $[(CH_3)_4N]_2[Zn(SC_6H_5)_4]$ constant at 50.0 mM, we introduced varied quantities of $(CH_3)_4N(SC_6H_5)$, affording solutions with $(CH_3)_4N(SC_6H_5)$ to $[(CH_3)_4N]_2[Zn(SC_6H_5)_4]$ ratios of 1:1, 5:1, 7.5:1, and 10:1. The ^1H NMR spectra of these solutions are shown in Figure 8.

Peak broadening persists in $(CH_3)_4N(SC_6H_5)$ and $[(CH_3)_4N]_2[Zn(SC_6H_5)_4]$ mixtures with ratios of 1:1, 5:1, 7.5:1, and 10:1. The spectra of these mixtures, however, exhibit two sets of benzenethiolate resonances. For example, the 5:1 solution displays one set of phenyl proton resonances at 6.41 (para), 6.66 (meta), and 7.01 (ortho) ppm and another at 6.61 (para), 6.74 (meta), and 7.44 (ortho) ppm (Figure 8C). The separation into two discrete resonance sets, in addition to a slightly enhanced degree of peak splitting, is most pronounced at the higher ratios (Figure 8C, D). When $(CH_3)_4N(PF_6)$ was added to a solution of $[(CH_3)_4N]_2[Zn(SC_6H_5)_4]$ to increase the amount of ion paired zinc tetrathiolate, the benzenethiolate ^1H NMR resonances become somewhat sharper than in a solution of $[(CH_3)_4N]_2[Zn(SC_6H_5)_4]$ alone (data not shown). This sharpening is due to increased amounts of ion-paired complex and less ligand dissociation from this ion-paired complex than the $[Zn(SC_6H_5)_4]^{2-}$ dianion (eq 10). We therefore assign the two sets of benzenethiolate resonances in $[(CH_3)_4N]_2[Zn(SC_6H_5)_4]$ solutions

Scheme 3

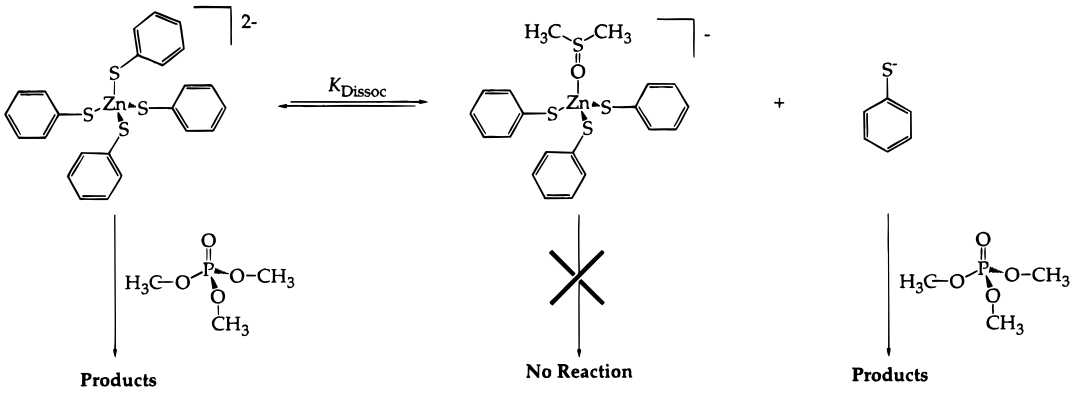

Scheme 4

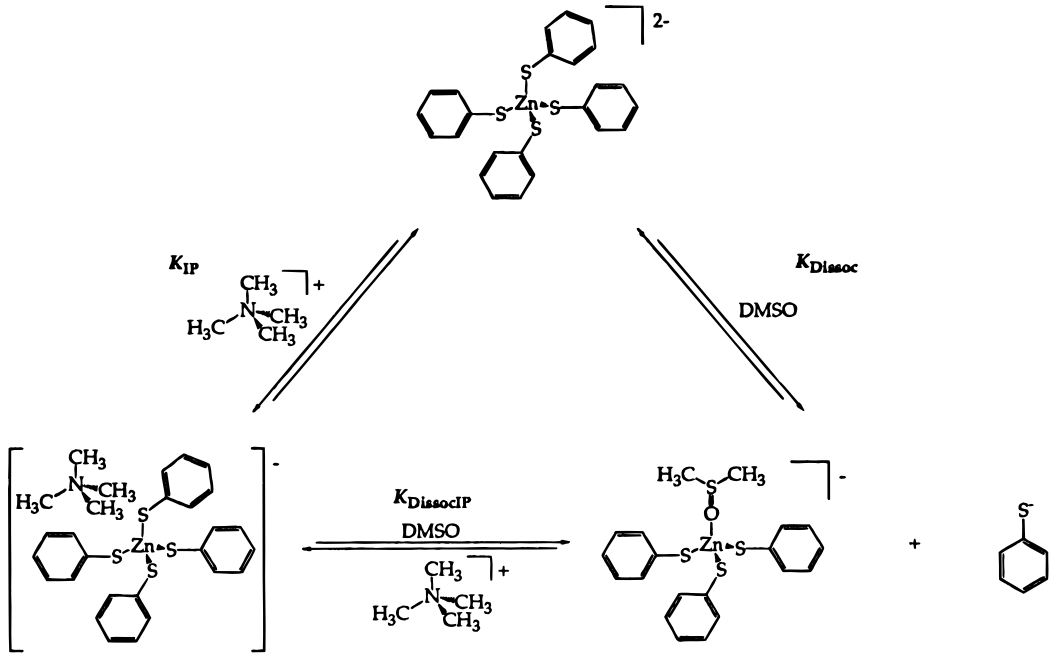

with added $(CH_3)_4N(SC_6H_5)$ to $\{[(CH_3)_4N][Zn(SC_6H_5)_4]\}^-$ and $C_6H_5S^-$. The upfield set of peaks have similar shifts to those of $(CH_3)_4N(SC_6H_5)$ and are so assigned.

From the concentrations of $\{[(CH_3)_4N][Zn(SC_6H_5)_4]\}^-$ and $C_6H_5S^-$ obtained from integrating the ^1H NMR peaks, a value for the ligand dissociation equilibrium constant from the ion paired complex, $K_{DissocIP}$ (eq 9), was computed. The $[\{Zn(SC_6H_5)_3(DMSO)\}^-]$ and $[(CH_3)_4N^+]_{free}$ concentrations were obtained in the following manner. The desired $[(CH_3)_4N^+]_{free}$ value is given by eq 11, in which both

$$[(CH_3)_4N^+]_{free} = [(CH_3)_4N^+]_{total} - [\{[(CH_3)_4N][Zn(SC_6H_5)_4]\}^-] \quad (11)$$

$[(CH_3)_4N^+]_{total}$ and $[\{[(CH_3)_4N][Zn(SC_6H_5)_4]\}^-]$ are known quantities. Under the conditions of added $(CH_3)_4N(SC_6H_5)$, the $[\{Zn(SC_6H_5)_3(DMSO)\}^-]$ concentration is determined from eq 12, in which $[Zn^{2+}]_{total}$ and $[\{[(CH_3)_4N][Zn(SC_6H_5)_4]\}^-]$ are

$$[\{Zn(SC_6H_5)_3(DMSO)\}^-] = [Zn^{2+}]_{total} - [\{[(CH_3)_4N][Zn(SC_6H_5)_4]\}^-] \quad (12)$$

known. Note that this expression does not include non-ion-paired zinc tetrathiolate, $[\{Zn(SC_6H_5)_4\}^{2-}]_{free}$, since the appearance of separate ^1H NMR resonances for $\{[(CH_3)_4N][Zn(SC_6H_5)_4]\}^-$ and $C_6H_5S^-$ in solutions of $[(CH_3)_4N]_2[Zn(SC_6H_5)_4]$ with added $(CH_3)_4N(SC_6H_5)$ indicates that most of the zinc tetrathiolate is ion paired. If such is not the case, the concentration of $\{[(CH_3)_4N][Zn(SC_6H_5)_4]\}^-$ may be overestimated, resulting in an underestimate of the $K_{DissocIP}$ value (eq 9). In any event, we now have all the concentrations required to compute $K_{DissocIP}$ by eq 9 and, consequently, can set a *lower limit* for the desired equilibrium constant for ligand loss from $[Zn(SC_6H_5)_4^{2-}]_{free}$, K_{Dissoc} (eq 10).

Substitution of eqs 11 and 12 into eq 9 provides an expression for $K_{DissocIP}$ in terms of known quantities (eq 13), where

$$K_{DissocIP} = \{([Zn^{2+}]_{total} - [(N^+ZnS_4)^-])[C_6H_5S^-] \times ([(CH_3)_4N^+]_{total} - [(N^+ZnS_4)^-])\}/[(N^+ZnS_4)^-] \quad (13)$$

$[(N^+ZnS_4)^-] = [\{[(CH_3)_4N][Zn(SC_6H_5)_4]\}^-]$. Measured concentrations of $\{[(CH_3)_4N][Zn(SC_6H_5)_4]\}^-$ and $[C_6H_5S^-]$ from the solutions with $(CH_3)_4N(SC_6H_5)$ to $[(CH_3)_4N]_2[Zn(SC_6H_5)_4]$ ratios of 5:1, 7.5:1, and 10:1 were used in eq 13 to obtain three independent values of $K_{DissocIP}$. An average of these results, reflecting one standard deviation, provides a $K_{DissocIP}$ value of $(1.0 \pm 0.9) \times 10^{-2}$ M (Table 2).

Reactivity of $[(CH_3)_4N]_2[Zn(SC_6H_5)_4]$ Due to Dissociated $C_6H_5S^-$. With this $K_{DissocIP}$ value, we have a lower limit for

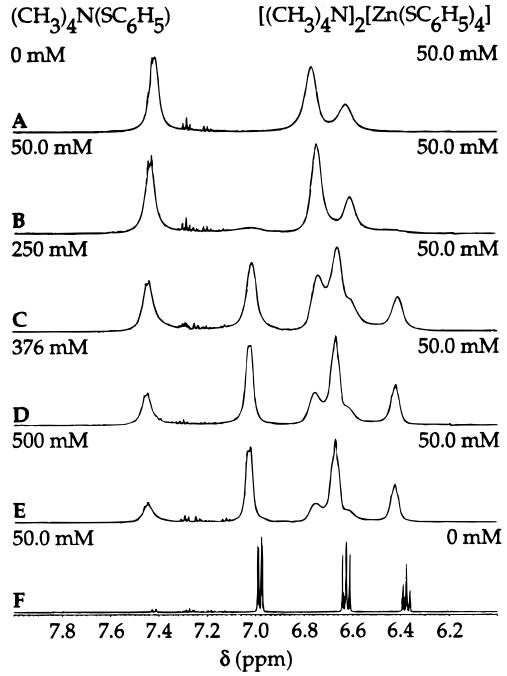

Figure 8. ^{1}H NMR spectra of 50.0 mM $[(CH_3)_4N]_2[Zn(SC_6H_5)_4]$ (A), 50.0 mM $(CH_3)_4N(SC_6H_5)$ and 50.0 mM $[(CH_3)_4N]_2[Zn(SC_6H_5)_4]$ (1:1 ratio) (B), 250 mM $(CH_3)_4N(SC_6H_5)$ and 50.0 mM $[(CH_3)_4N]_2[Zn(SC_6H_5)_4]$ (5:1 ratio) (C), 376 mM $(CH_3)_4N(SC_6H_5)$ and 50.0 mM $[(CH_3)_4N]_2[Zn(SC_6H_5)_4]$ (7.5:1 ratio) (D), 500 mM $(CH_3)_4N(SC_6H_5)$ and 50.0 mM $[(CH_3)_4N]_2[Zn(SC_6H_5)_4]$ (10:1 ratio) (E), and 50.0 mM $(CH_3)_4N(SC_6H_5)$ (F) in DMSO-d_6.

dissociation from the non-ion paired zinc tetrathiolate species $[Zn(SC_6H_5)_4^{2-}]_{free}$. Thus, K_{Dissoc} is $\geq(1.0 \pm 0.9) \times 10^{-2}$ M (Table 2). Pseudo-first-order kinetic studies of the reaction of $[(CH_3)_4N]_2[Zn(SC_6H_5)_4]$ with $(CH_3O)_3PO$ at 5.0 mM and 1.0 mM afford a rate constant of $(8.2 \pm 0.6) \times 10^{-5}$ s^{-1} (Table 1). We now consider how much of this reactivity might be due to dissociated benzenethiolate. From the lower limit of K_{Dissoc}, we can obtain a lower limit of benzenethiolate dissociated from zinc. As shown in eq 14 and Scheme 3, the concentrations of

$$[C_6H_5S^-]_{Zn} = [\{Zn(SC_6H_5)_3(DMSO)\}^-] \qquad (14)$$

dissociated benzenethiolate and $[Zn(SC_6H_5)_3(DMSO)]^-$ are equal. This equality and the expression for the concentration of starting zinc complex, $[Zn^{2+}]_{start}$ (eq 15), can be substituted

$$[Zn^{2+}]_{start} = [\{Zn(SC_6H_5)_4\}^{2-}]_{free} + [\{Zn(SC_6H_5)_3(DMSO)\}^-] \qquad (15)$$

into eq 8, which defines K_{Dissoc}. Rearrangement affords eq 16,

$$[C_6H_5S^-] = \frac{-K_{Dissoc} \pm (K_{Dissoc}^{\ 2} + 4\,K_{Dissoc}[Zn^{2+}]_{start})^{1/2}}{2} \qquad (16)$$

derived in Appendix S3. Note that $[Zn^{2+}]_{start}$ is $[Zn^{2+}]_{total}$ exclusive of the ion paired tetrathiolate, $\{[(CH_3)_4N][Zn(SC_6H_5)_4]\}^-$. The low, 5.0 mM concentration of $[(CH_3)_4N]_2[Zn(SC_6H_5)_4]$ used in this analysis was chosen to minimize ion-pairing such that only $[Zn(SC_6H_5)_4^{2-}]_{free}$ and $[Zn(SC_6H_5)_3(DMSO)]^-$ concentrations were significant. By using the lower limit for K_{Dissoc} and a $Zn^{2+}{}_{start}$ concentration of 5.0 mM from the kinetic runs of interest, a minimum $[C_6H_5S^-]_{Zn}$ concentration of 3.7 ± 0.4 mM was obtained. Relative to the starting $[(CH_3)_4N]_2[Zn(SC_6H_5)_4]$ concentration of 5.0 mM, this lower limit is significant and warrants further examination.

Kinetic studies of the reaction between 5.0 mM $(CH_3)_4N(SC_6H_5)$ and 1.0 mM $(CH_3O)_3PO$ provided a pseudo-first-order rate constant of $(1.1 \pm 0.3) \times 10^{-4}$ s^{-1} (Table 1). Since the reaction of $[(CH_3)_4N]_2[Zn(SC_6H_5)_4]$ with $(CH_3O)_3PO$ is second-order (eq 6), it is reasonable to assume that the reaction between $(CH_3)_4N(SC_6H_5)$ and $(CH_3O)_3PO$ is also second-order and follows the rate law shown in eq 17. With

$$-\frac{d[C_6H_5S^-]}{dt} = k_{PhS}\,[C_6H_5S^-][(CH_3O)_3PO] \qquad (17)$$

this assumption, the pseudo-first-order rate constant for benzenethiolate, k_{obs}, depends upon the second-order rate constant (k_{PhS}) and concentration of benzenethiolate ($[C_6H_5S^-]$), as indicated in eq 18. From the pseudo-first-order rate constant

$$k_{obs} = k_{PhS}\,[C_6H_5S^-] \qquad (18)$$

of $(1.1 \pm 0.3) \times 10^{-4}$ s^{-1} (Table 1) and eq 18, the second-order rate constant for benzenethiolate reacting with $(CH_3O)_3PO$, k_{PhS}, is $(2.2 \pm 0.6) \times 10^{-2}$ M^{-1} s^{-1} (Table 2). From this value, the 3.7 ± 0.4 mM lower limit of benzenethiolate concentration derived from $[(CH_3)_4N]_2[Zn(SC_6H_5)_4]$ and eqs 7 and 18, we compute a calculated k_{obs} value, k_{calc}, of $(8 \pm 4) \times 10^{-5}$ s^{-1} (Table 2). This calculated value compares quite favorably with the measured pseudo-first-order rate constant of $(8.2 \pm 0.6) \times 10^{-5}$ s^{-1} for the reaction of 5.0 mM $[(CH_3)_4N]_2[Zn(SC_6H_5)_4]$ and 1.0 mM $(CH_3O)_3PO$ (Table 1). *We therefore conclude that dissociated thiolate is accountable for all the measured reactivity of $[(CH_3)_4N]_2[Zn(SC_6H_5)_4]$.* Scheme 5 summarizes the solution behavior of $[(CH_3)_4N]_2[Zn(SC_6H_5)_4]$ with respect to ion pairing, ligand dissociation, and reactivity with $(CH_3O)_3PO$.

Metal Ion Variation. In order to address the question of why zinc may have evolved for repair of alkyl phosphotriesters by Ada, we explored the reactivity of cobalt(II) and cadmium(II) tetrathiolate complexes. Both $[(CH_3)_4N]_2[Co(SC_6H_5)_4]$ and $[(CH_3)_4N]_2[Cd(SC_6H_5)_4]$ react with $(CH_3O)_3PO$. Products from reaction with the cobalt complex are similar to those obtained in a stoichiometric reaction of $[(CH_3)_4N]_2[Zn(SC_6H_5)_4]$ with $(CH_3O)_3PO$. The thioether $CH_3SC_6H_5$ is not coordinated to the cobalt center, as indicated by ^{1}H NMR resonances, which were identical to those of a genuine sample. The phosphate $(CH_3O)_2PO_2^-$ appears to be in an equilibrium between metal-bound and free states, as demonstrated by a broad ($\Delta\nu_{1/2} =$ 238 Hz) $^{31}P\{^1H\}$ NMR resonance similar to that observed in the zinc reaction. As indicated in Table 1, $[(CH_3)_4N]_2[Co(SC_6H_5)_4]$ exhibits a pseudo-first-order rate constant significantly less than that of $[(CH_3)_4N]_2[Zn(SC_6H_5)_4]$.

Products for a 1:1 reaction between $[(CH_3)_4N]_2[Cd(SC_6H_5)_4]$ and $(CH_3O)_3PO$ are slightly different than for the zinc and cobalt complexes. Again, the methylated product $CH_3SC_6H_5$ is not coordinated to the $\{Cd(SC_6H_5)_3\}^-$ product moiety according to ^{1}H NMR spectroscopy. A sharp ($\Delta\nu_{1/2} = 3.6$ Hz) $^{31}P\{^1H\}$ NMR product peak, however, differs from the broad resonances observed following the zinc and cobalt reactions. This sharp peak establishes that $(CH_3O)_2PO_2^-$ is not in an equilibrium between cadmium-bound and dissociated states. Currently, we cannot determine whether $(CH_3O)_2PO_2^-$ is coordinated to cadmium or free. The ^{113}Cd NMR spectrum of a 510 mM $[(CH_3)_4N]_2[Cd(SC_6H_5)_4]$ solution in DMSO-d_6 exhibits a peak at 569 ppm, in good agreement with literature values for similar complexes.[23,24] A ^{113}Cd NMR spectrum following a stoichio-

(23) Coleman, J. E. In *Methods in Enzymology*; Riordan, J. F., Vallee, B. L., Eds.; Academic Press: Boston, MA 1993; Vol. 227, pp 16−43.

Scheme 5

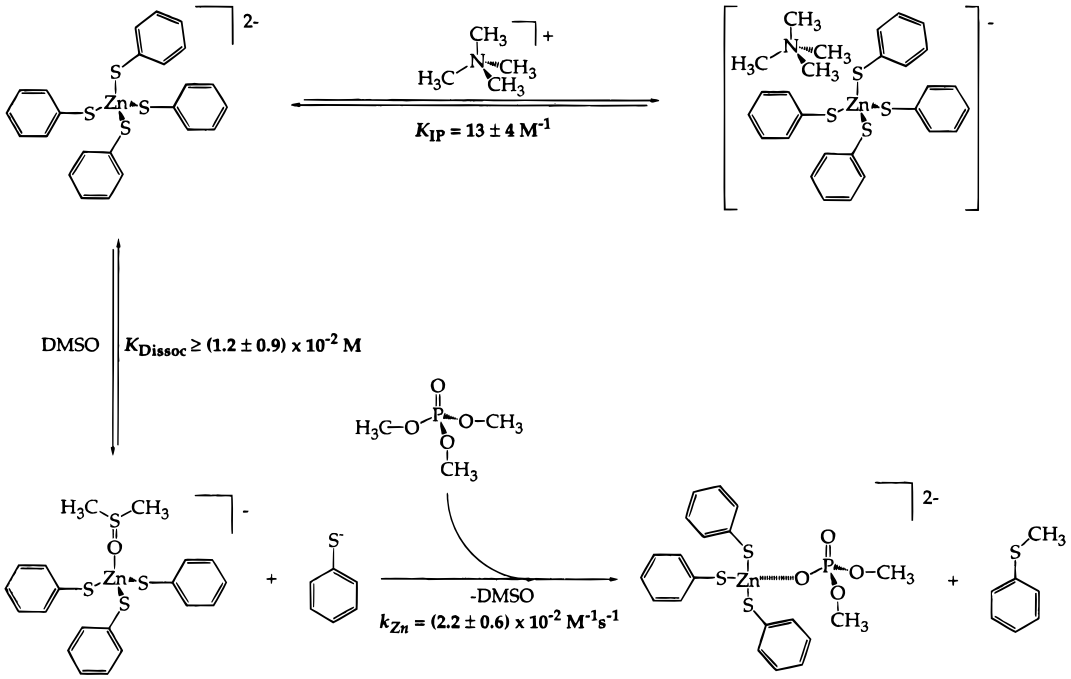

metric reaction between 510 mM $[(CH_3)_4N]_2[Cd(SC_6H_5)_4]$ and 510 mM $(CH_3O)_3PO$, however, displays no signal. This lack of signal in a ^{113}Cd NMR spectrum has precedence and is often attributed to exchange broadening.[24−26] The cadmium form of the methyl phosphotriester repair active 10 kDa N-terminal fragment of Ada (Cd−*N*-Ada10) also displays no ^{113}Cd NMR resonance after alkyl phosphotriester repair.[8] As is the case with the cobalt tetrathiolate complex, reaction of $[(CH_3)_4N]_2[Cd(SC_6H_5)_4]$ and $(CH_3O)_3PO$ proceeds with a pseudo-first-order rate constant less than that of $[(CH_3)_4N]_2[Zn(SC_6H_5)_4]$ (Table 1).

Discussion

Mechanism of Demethylation of Trimethyl phosphate by Zinc Model Complexes: Comparison to Ada. The present results illustrate methyl transfer from a phosphotriester to a zinc thiolate model in a reaction that mimics Ada repair of DNA methyl phosphotriesters. Repair of methyl phosphotriesters in Ada, therefore, is probably an intrinsic property of the $[Zn(S\text{-cys})_4]^{2-}$ moiety, unlike Ada repair of alkylated base lesions such as O^6-methylguanine and O^4-methylthymine, which requires a structurally complex system of amino acid residues hydrogen bonded to the substrate.[13] Products of the reaction between $[(CH_3)_4N]_2[Zn(SC_6H_5)_4]$ and $(CH_3O)_3PO$ are not completely analogous to those found in the protein system, however. The methylated thiolate $CH_3SC_6H_5$ does not remain coordinated, whereas methylated Cys69 is apparently metal-bound in both the zinc and cadmium forms of Ada.[8,9] The phosphate product $(CH_3O)_2PO_2^-$ is partially coordinated in the model, whereas the protein presumably releases the repaired substrate to permit genome binding for transcriptional regulation.[27−31]

The reaction between $[(CH_3)_4N]_2[Zn(SC_6H_5)_4]$ and $(CH_3O)_3PO$ is second-order, first-order with respect to each reagent, with a rate constant of $(1.6 \pm 0.3) \times 10^{-2}\ M^{-1}\ s^{-1}$ at 24.5 (± 0.6) °C (Table 2). By comparison, Ada repair of a methyl phosphotriester lesion occurs in aqueous buffer at 4 °C with a second-order rate constant of $2.8 \times 10^2\ M^{-1}\ s^{-1}$.[32] It is not surprising that the protein effects methyl transfer with a rate constant higher than that of a model complex. Proteins evolve to provide optimal substrate binding, orientation, and transition state stabilization.[33,34] In addition, there are many differences between the protein and our synthetic analogs. In this study, we employed aromatic thiolates, which are less basic than the aliphatic cysteine residues of Ada.[35] Solvent differences (H_2O vs DMSO) and the energetics of $(CH_3O)_3PO$ rather than a DNA methyl phosphotriester are additional factors which contribute to kinetic differences between the protein and model chemistry. NMR investigations of the active 10 kDa N-terminal Ada protein fragment containing the $[Zn(S\text{-cys})_4]^{2-}$ center (*N*-Ada10) revealed that the residue responsible for alkyl phosphotriester repair (Cys69) is bound to zinc.[14,15] The cadmium-substituted form of this protein fragment, however, exhibited no observable ^1H-^{113}Cd scalar coupling involving the β-protons of Cys69.[8,14] By contrast, such scalar coupling was observed for the three other cysteine ligands of zinc (Cys38, Cys 42, and Cys72). Reactions of *N*-Ada10 with the methylating agent CH_3I demonstrated that, not only is Cys69 more nucleophilic than the other cysteine ligands, but Cys69 is the most nucleophilic site in the protein fragment.[36] Our model studies indicate that metal-

(24) Summers, M. F. *Coord. Chem. Rev.* **1988**, *86*, 43−134.
(25) Keller, A. D.; Drakenberg, T.; Briggs, R. W.; Armitage, I. M. *Inorg. Chem.* **1985**, *24*, 1170−1174.
(26) Armitage, I. M.; Otvos, J. D. In *Biological Magnetic Resonance*; Berliner, L. J., Reuben, J., Eds.; Plenum Press: New York, 1984; Vol. 4, pp 79−144.
(27) Saget, B. M.; Walker, G. C. *Proc. Natl. Acad. Sci. U.S.A.* **1994**, *91*, 9730−9734.
(28) Shevell, D. E.; Friedman, B. M.; Walker, G. C. *Mutat. Res.* **1990**, *233*, 53−72.
(29) Nakabeppu, Y.; Sekiguchi, M. *Proc. Natl. Acad. Sci. U.S.A.* **1986**, *83*, 6297−6301.
(30) Teo, I.; Sedgwick, B.; Kilpatrick, M. W.; McCarthy, T. V.; Lindahl, T. *Cell* **1986**, *45*, 315−324.
(31) Volkert, M. R.; Nguyen, D. C. *Proc. Natl. Acad. Sci. U.S.A.* **1984**, *81*, 4110−4114.
(32) Myers, L. C.; Jackow, F.; Verdine, G. L. *J. Biol. Chem.* **1995**, *270*, 6664−70.
(33) Lippard, S. J.; Berg, J. M. *Principles of Bioinorganic Chemistry*; University Science Books: Mill Valley, CA, 1994.
(34) Fersht, A. *Enzyme Structure and Mechanism*; 2nd ed.; W. H. Freeman and Co.: New York, 1985.
(35) Crampton, M. R. In *The Chemistry of the Thiol Group*; Patai, S., Ed.; John Wiley and Sons: New York, 1974; pp 379−415.

bound thiolates must have rate constants for methyl transfer less than that of free thiolate (Table 1). Combining these results with those for the protein fragment, we propose a repair mechanism for Ada involving the Cys69 residue in equilibrium between coordinated and free states. The zinc-bound state prevents protonation while the transiently dissociated state presents a thiolate nucleophile to the alkyl phosphotriester lesion for alkyl transfer. This mechanism is consistent with a proposal in which the Cys69 thiolate is in equilibrium between a zinc-bound state and one hydrogen bonded to the proximal (∼3.2 Å) backbone amide N−H of Gln73.[36] In such a case, the thiolate "in flight" between the zinc and the amide hydrogen may serve as the repair active nucleophile.

Recently, a zinc-dependent alkyl transfer reaction was discovered in *E. coli* cobalamin-independent methionine synthase, which catalyzes methionine formation from methyltetrahydrofolate and homocysteine.[37] Methylation of the homocysteine sulfur appears to require transient thiolate binding of this substrate to zinc in the enzyme. The present results strongly support the proposal[37] that the probable role of zinc in this system is to create or preserve a thiolate nucleophile for methylation.

Other Zinc Thiolate Complexes. The reactivity of complexes representing $[Zn(S\text{-cys})_4]^{2-}$, $[Zn(S\text{-cys})_3(N\text{-his})]^-$, and $[Zn(S\text{-cys})_2(N\text{-his})_2]$ protein sites has also been explored. All three compounds, $[(CH_3)_4N]_2[Zn(SC_6H_5)_4]$, $[(CH_3)_4N][Zn(SC_6H_5)_3(MeIm)]$, and $[Zn(SC_6H_5)_2(MeIm)_2]$, react with $(CH_3O)_3PO$ to yield products analogous to those found in the parent $[(CH_3)_4N]_2[Zn(SC_6H_5)_4]$ system. Pseudo-first-order rate constants of these reactions follow the trend $[(CH_3)_4N]_2[Zn(SC_6H_5)_4] > [(CH_3)_4N][Zn(SC_6H_5)_3(MeIm)] > [Zn(SC_6H_5)_2(MeIm)_2]$ (Table 1). The low rate constant for reaction of $[Zn(SC_6H_5)_2(MeIm)_2]$ indicates that $[Zn(S\text{-cys})_2(N\text{-his})_2]$ sites possess a very low level of nucleophilicity. This lack of reactivity is consistent with the use of the $[Zn(S\text{-cys})_2(N\text{-his})_2]$ center for structural purposes and may account in part for the prominence of this motif in nature.[38−41]

Sharp and well-resolved ^{1}H NMR peaks (Figure 7) and low conductivity readings (Figure 4) for the neutral complex $[Zn(SC_6H_5)_2(MeIm)_2]$ indicate little benzenethiolate dissociation. If, as suggested, all reactivity of $[(CH_3)_4N]_2[Zn(SC_6H_5)_4]$ is due to a dissociated thiolate, the lesser degree of ligand dissociation from $[(CH_3)_4N][Zn(SC_6H_5)_3(MeIm)]$ should yield a lower level of reactivity toward trimethyl phosphate. Such is indeed the case, as indicated by the low k_{obs} value in reaction with $(CH_3O)_3PO$ (Table 1). If the dianionic $[Zn(S\text{-cys})_4]^{2-}$ protein center can dissociate a ligand readily, as suggested for Ada, a $[Zn(S\text{-cys})_3(N\text{-his})]^-$ site would be less likely to do so. Thiolate loss from the $[Zn(S\text{-cys})_2(N\text{-his})_2]$ would be even more unlikely. Our results suggest that, if the three zinc-ligating cysteines of Ada other than Cys69 were to be mutated to histidine residues, rate constants for alkyl phosphotriester repair would diminish as the number of histidine ligands increased.

Comparison to Cobalt and Cadmium Analogs. The selection of zinc by Ada as the metal ion of choice for the alkyl phosphotriester repair site could have occurred for a variety of reasons.[33,38] Redox active ions such as cobalt(II) and iron(II) would be poor choices owing to the possibility of redox damage to the DNA substrate or protein. The present results show that metal ions other than zinc may be less adept at methyl phosphotriester repair. In particular, the cobalt(II) and cadmium(II) complexes $[(CH_3)_4N]_2[Co(SC_6H_5)_4]$ and $[(CH_3)_4N]_2[Cd(SC_6H_5)_4]$ react with $(CH_3O)_3PO$ with rate constants lower than that of the zinc analog $[(CH_3)_4N]_2[Zn(SC_6H_5)_4]$ (Table 1). Thus, not only is zinc redox inactive, it may also provide a higher rate constant for alkyl phosphotriester repair than other metal ions. The cadmium form of *N*-Ada10 repairs a methyl phosphotriester lesion with a second-order rate constant one quarter the value of the zinc form.[32] A similar trend is observed with model chemistry, methyl transfer to $[(CH_3)_4N]_2[Cd(SC_6H_5)_4]$ occurring with a pseudo-first-order rate constant almost one-third that of the zinc complex $[(CH_3)_4N]_2[Zn(SC_6H_5)_4]$ (Table 1). We interpret these differences in reactivity to varying degrees of ligand dissociation. Cadmium exhibits a higher affinity for sulfur donors than zinc, as evidenced by literature binding constants for thiourea.[42,43] An analogous heightened ability of cadmium to bind the benzenethiolate ligand will result in less dissociated ligand and, hence, decreased reactivity. Cobalt(II) ions also display higher thiourea binding constants than zinc.[42,43] This finding correlates well with our data, in which the rate constant of methyl transfer for the cobalt complex $[(CH_3)_4N]_2[Co(SC_6H_5)_4]$ is less than that found for the analogous zinc complex.

The sulfur-based reactions of metal thiolate complexes have been studied extensively.[44−50] Comprehensive reactant and product characterizations were completed in such studies, but the exact identities of reactive species have remained elusive. To the best of our knowledge, the present investigation is the first in which the reaction kinetics of a simple thiolate and its metal complexes are compared. Although ligand dissociation makes direct comparisons between metal-bound and free thiolate difficult, our kinetic results reveal the general trend that metal complexes have decreased reactivity, and hence less nucleophilicity, than the metal-free counterpart. The proposed phenomenon of metal-enhanced nucleophilicity is not observed in our work.[15,49] Coordination to a metal ion withdraws electron density from the sulfur and reduces thiolate nucleophilicity.

Conclusions

A functional model for Ada repair of alkyl phosphotriester DNA damage has been developed in which methyl transfer occurs from $(CH_3O)_3PO$ to $[(CH_3)_4N]_2[Zn(SC_6H_5)_4]$. The simple thiolate $(CH_3)_4N(SC_6H_5)$ is also capable of methyl transfer, whereas the thiol C_6H_5SH is inactive. From these observations, we infer that zinc binding of Cys69, the Ada residue responsible for alkyl phosphotriester repair, prevents protonation and maintains this residue in the repair-active

(36) Myers, L. C.; Wagner, G.; Verdine, G. L. *J. Am. Chem. Soc.* **1995**, *117*, 10749−10750.
(37) Gonzalez, J. C.; Peariso, K.; Penner-Hahn, J. E.; Matthews, R. G. *Biochemistry* **1996**, *35*, 12228−12234.
(38) Berg, J. M.; Shi, Y. *Science* **1996**, *271*, 1081−1085.
(39) Klug, A.; Schwabe, J. W. R. *FASEB J.* **1995**, *9*, 597−604.
(40) Rhodes, D.; Klug, A. *Sci. Am.* **1993**, *268*, 56−65.
(41) Vallee, B. L.; Auld, D. S. *Acc. Chem. Res.* **1993**, *26*, 543−551.
(42) Martell, A. E.; Smith, R. M. *Critical Stability Constants*; Plenum Press: New York, 1982; Vol. 5, First Supplement.
(43) Martell, A. E.; Smith, R. M. *Critical Stability Constants*; Plenum Press: New York, 1977; Vol. 3.
(44) Buonomo, R. M.; Font, I.; Maguire, M. J.; Reibenspies, J. H.; Tuntulani, T.; Darensbourg, M. Y. *J. Am. Chem. Soc.* **1995**, *117*, 963−973.
(45) Ram, M. S.; Riordan, C. G.; Ostrander, R.; Rheingold, A. L. *Inorg. Chem.* **1995**, *34*, 5884−5892.
(46) Wilker, J. J.; Gelasco, A.; Pressler, M. A.; Day, R. O.; Maroney, M. J. *J. Am. Chem. Soc.* **1991**, *113*, 6342−6343.
(47) Mills, D. K.; Reibenspies, J. H.; Darensbourg, M. Y. *Inorg. Chem.* **1990**, *29*, 4364−4366.
(48) Lindoy, L. F.; Busch, D. H. *Inorg. Chem.* **1974**, *13*, 2494−2498.
(49) Blinn, E. L.; Busch, D. H. *J. Am. Chem. Soc.* **1968**, *90*, 4280−4285.
(50) Busch, D. H.; Jr., J. A. B.; Jicha, D. C.; Thompson, M. J.; Morris, M. L. In *Reactions of Coordinated Ligands and Homogeneous Catalysis*; Busch, D. H., Ed.; American Chemical Society: Washington DC, 1963; Vol. 37, pp 125−142.

thiolate state. Conductivity, kinetic, and ^{1}H NMR experiments show that the complex $[(CH_3)_4N]_2[Zn(SC_6H_5)_4]$ forms ion pairs in DMSO solution with an equilibrium constant for ion pairing, K_{IP}, of 13 ± 4 M^{-1} (Table 2). The reaction between solvated $[Zn(SC_6H_5)_4]^{2-}$ and $(CH_3O)_3PO$ is a second-order process, first-order with respect to each reagent, and exhibits a second-order rate constant, k_{Zn}, of $(1.6 \pm 0.3) \times 10^{-2}$ M^{-1} s^{-1} (Table 2). The zinc tetrathiolates $[Zn(SC_6H_5)_4]^{2-}$ and $\{[(CH_3)_4N][Zn(SC_6H_5)_4]\}^-$ undergo appreciable degrees of ligand dissociation. Addition of $(CH_3)_4N(SC_6H_5)$ to solutions of $[(CH_3)_4N]_2[Zn(SC_6H_5)_4]$ both increased the formation of ion pairs with the zinc tetrathiolate dianion and drove the dissociation equilibria toward the bound states increasing the concentration of $\{[(CH_3)_4N][Zn(SC_6H_5)_4]\}^-$. Examination of these solutions by ^{1}H NMR spectroscopy yielded an equilibrium constant for dissociation from $\{[(CH_3)_4N][Zn(SC_6H_5)_4]\}^-$, $K_{DissocIP}$, of $(1.0 \pm 0.9) \times 10^{-2}$ M. This equilibrium constant is the lower limit for the equilibrium constant for ligand loss from $[Zn(SC_6H_5)_4]^{2-}$, K_{Dissoc}. By using this lower limit, the reactivity of $[(CH_3)_4N]_2[Zn(SC_6H_5)_4]$ was ascribed completely to dissociated benzenethiolate.

Metal complexes representing alternative protein sites were examined for reactivity with $(CH_3O)_3PO$. Pseudo-first-order rate constants provided the following trend: $[(CH_3)_4N]_2[Zn(SC_6H_5)_4] > [(CH_3)_4N][Zn(SC_6H_5)_3(MeIm)] > [Zn(SC_6H_5)_2(MeIm)_2]$. These data suggest that $[Zn(S\text{-cys})_4]^{2-}$ is the optimal zinc center for alkyl phosphotriester repair and that $[Zn(S\text{-cys})_2(N\text{-his})_2]$ sites lack an appreciable degree of nucleophilicity. Cobalt and cadmium tetrathiolate complexes also react with $(CH_3O)_3PO$, but with rate constants less than that of the zinc analog. These differences in reactivity of the metal thiolate complexes are attributed to varied degrees of thiolate dissociation. On the basis of our results and published studies on the protein, we propose a mechanism for alkyl phosphotriester repair in Ada where a transiently dissociated Cys69 ligand is the nucleophile responsible for accepting an alkyl moiety from the DNA alkyl phosphotriester lesion. The zinc-bound state prevents protonation and deactivation of the cysteine thiolate nucleophile. Finally, our kinetic data indicate that metal thiolate moieties display generally decreased nucleophilicity relative to that of free thiolates.

Acknowledgment. This research was supported by Grant CA34992 from the National Cancer Institute. We are grateful to A. Bakač and S. Herold for many valuable discussions. We thank R. Matthews for kindly providing a preprint of ref 37. J.J.W. is a predoctoral trainee under NCI Training Grant CA09112.

Supporting Information Available: Text giving derivations of eqs 4, 5, and 16 (4 pages). Ordering information is given on any current masthead page.

IC961082O